J Therm Anal Calorim (2012) 109:63–67
DOI 10.1007/s10973-011-1366-3

# Influence of solid-phase ferritization method on phase composition of lithium-zinc ferrites with various concentration of zinc

**A. P. Surzhikov · A. M. Pritulov · E. N. Lysenko · A. N. Sokolovskii · V. A. Vlasov · E. A. Vasendina**

Received: 30 November 2010 / Accepted: 20 January 2011 / Published online: 12 February 2011


**Abstract** Methods of X-ray phase analysis (XRPA) and differential thermogravimetry in a magnetic field (DTG (M)) are used to investigate the phase composition of $Li_{0.5(1-x)}Fe_{2.5-0.5x}Zn_xO_4$ ($x_{Zn} = 0.2$, 0.4, and 0.6) ferrite spinels synthesized at a temperature of 700 °C during 120 min by thermal annealing of a reagent mixture in a furnace and heating of the mixture using high-power beam of accelerated electrons with energy of 2.4 MeV. Thermal ferritization of all compositions leads to the formation of phases whose composition is close to simple monoferrites. Lithium–zinc ferrite phases are formed during annealing under electron irradiation. It is concluded that the rate of controllable diffusion interaction of monoferrite phases significantly increases under conditions of high-power electron irradiation.

**Keywords** Li–Zn ferrite · Pulsed electron beam · Radiation-thermal method · Solid-state synthesis · DTG(M) curves

## Introduction

High sensitivity of the magnetic parameters to the chemical homogeneity of ferrites stimulates a search for and development of methods capable of significant improvement of homogeneity of synthesized products. This problem is especially urgent for solid-phase synthesis of multicomponent ferrites widespread in industry. This is explained by the fact that the mechanical mixture used to synthesize multicomponent ferrites comprises several individual oxides, and ferrite is fist formed in places of their contact. Therefore, the primary products of the solid-phase reaction are typically monoferrites together with solid solutions of oxides. All this leads to the fact that primary solid-phase reaction products differ by chemical composition whose fluctuations are retained during further annealing.

By the present time, the main reasons for chemical inhomogeneity of ferrite powders are well known. The methods of chemical homogenization developed for their control are complicated for practical implementation, have low efficiency, and are not irreproachable from the ecological viewpoint [1, 2].

Other approaches to a solution of this problem consist in the application of physical methods of reagent activation directly in the process of solid-phase synthesis [3, 4]. A highly efficient radiation-thermal (RT) method is among them. The method consists in heating of reaction mixtures using a high-power beam of accelerated electrons [5, 6]. It is the most versatile and simplest method of physical activation of solid-phase reactions. The efficiency of the RT method has been demonstrated, in particular, for reactions of solid-phase synthesis of pure [7] and doped lithium ferrites [8, 9].

In [9] it has been demonstrated that if $Li_{0.3}Fe_{2.3}Zn_{0.4}O_4$ lithium–zinc ferrite is synthesized by heating of the reaction mixture using an electron beam, the degree of mixture ferritization appears much greater than for thermal (T) annealing. Higher chemical homogeneity of the product of RT synthesis was also suggested. However, this assumption was based on indirect results and was not furnished with a convincing proof. Therefore, this work is aimed at proving higher homogeneity of the phase composition of samples synthesized by radiation-thermal method as against with traditional thermal synthesis.

A. P. Surzhikov · A. M. Pritulov · E. N. Lysenko · A. N. Sokolovskii (✉) · V. A. Vlasov · E. A. Vasendina
Tomsk Polytechnic University, 30, Lenin Avenue, Tomsk 634050, Russia
e-mail: s.a.n.gleiss@mail.ru

## Experimental

The lithium–zinc ferrite samples prepared from the mechanical mixture of $Li_2CO_3$–$Fe_2O_3$–ZnO powders were investigated. The zinc content in the mixtures was $x = 0.2$, 0.4, and 0.6. Mixtures of reagents were produced by weighing the required amount of pre-dried components and then were dry-mixed in an agate mortar with tenfold rubbing through a mesh with a 80-μm cell. The samples were compacted by single-ended cold pressing under a pressure of 200 MPa in the form of tablets with a diameter of 15 mm and thickness of 2 mm.

Thermal annealing of the samples was performed in a resistance furnace. Radiation-thermal annealing of samples was carried out in an ILU-6 pulse electron accelerator (Institute of Nuclear Physics of the SB RAS, Novosibirsk, Russia). The electron energy was 2.4 MeV, the beam current in the pulse was 400 mA, the pulse duration was 500 μs, and the pulse repetition frequency was 7–15 Hz. The average radiation dose was $\sim$5 kGy $s^{-1}$ at heating and $\sim$3 kGy $s^{-1}$ at isothermal annealing. The pulse radiation dose was 800 kGy $s^{-1}$. The samples were heated and the preset temperature regime was maintained at the expense of energy of decelerated electrons without external heat sources. The duration of non-isothermal stages (heating and cooling) did not exceed 3 min.

All ferritizing T and RT annealing procedures were performed in air at a temperature of 700 °C without intermediate grinding and mixing.

The phase composition of the examined samples was measured using an X-ray ARL X'TRA diffractometer with a Peltier Si(Li) semiconductor detector and Cu $K_\alpha$ radiation. XRD patterns were measured for $2\theta = (10–140)°$ with a scanning rate of 0.02° $s^{-1}$. Phases were identified using the PDF-4 powder database of the International Center for Diffraction Data (ICDD). The XRD patterns were processed by the full-profile analysis using the software *Powder Cell 2.5*.

The DTG(M) investigations were performed in the air atmosphere using an STA 449C Jupiter thermal analyzer (Netzsch, Germany). To control the sample magnetic state, permanent magnets ($H \sim 5$ Oe) were placed on the external side of the magnetic cell. Measurements were carried out in the mode of linear cooling at a rate of 20 °C $min^{-1}$ after the samples had been heated fast to a temperature of 800 °C. This measurement regime provided demagnetized initial state of the samples. It should be mentioned that the radiation-thermal method of registering magnetic phases in an external magnetic field was also used in [10] to investigate nanocrystalline and amorphous alloys.

## Results and discussion

Figure 1 shows T and RT XRD patterns of the synthesized samples with the indicated zinc contents in the mixture. After RT annealing, reflections of only spinel phases were detected for all structures. After T annealing, the XRD patterns represented a superposition of reflections from spinel phases and from particles of the initial ZnO and $Fe_2O_3$ oxides. Already a simple comparison of the XRD patterns demonstrates a considerably higher ferritization degree of the RT annealed mixtures for all investigated structures. Thus, the radiation-induced effect of intensification of the ferrite spinel synthesis was observed for lithium ferrites differently doped by zinc.

To analyze the phase composition of ferritized samples, a discrete batch of lithium–zinc ferrite phases with $x_{Zn} = 0$, 0.2, 0.4, 0.6, and 0.8 was prepared for the full-profile analysis. This batch of phases simulated a quasi-continuous distribution of $Li_{0.5(1-x)}Zn_xFe_{2.5-0.5x}O_4$ spinel phases that could be formed in different regions of the powder mixture within the X-ray beam. If necessary, the discrete distribution was extended through inclusion of phases of particles of the initial components. After fitting of the calculated and experimental XRD patterns, the phase concentrations and the parameters of their crystal lattices were determined. Then, using the dependence of the lithium–zinc ferrite lattice parameter on $x_{Zn}$ [11], the zinc content in the reference spinel phases used for calculations was refined. The refined $x_{Zn}$ values are actually weighted mean values which characterize the distribution of lithium–zinc ferrite spinel phases. The error caused by the replacement of the continuous distribution with the discrete one was leveled due to close values of the X-ray scattering cross-sections of the $Fe^{3+}$ and $Zn^{2+}$ ions.

Figure 2 shows the bar charts of the ferrite spinel phase composition in reaction mixtures ferritized in the T and RT annealing regimes at a temperature of 700 °C during 120 min. The dashed straight lines indicate the zinc content in the initial mixture. It can be seen that phases close to $Li_{0.5}Fe_{2.5}O_4$ and $ZnFe_2O_4$ monoferrites prevail after thermal annealing. The relative fractions of these phases depend on the relative zinc content in the initial mixture. Lithium monoferrite prevails in the composition with $x_{Zn} = 0.2$, and zinc monoferrite prevails in the mixture with $x_{Zn} = 0.6$. For intermediate zinc content $x_{Zn} = 0.4$, the lithium monoferrite and zinc concentrations ($x_{Zn} = 0.7$) are approximately identical. Spinels whose composition was close to that of the initial mixture was practically absent. Thus, under conditions of thermal ferritization at the examined temperature (700 °C) for the indicated process duration (120 min), the reaction of synthesis proceeded at the stage of monoferrite formation.

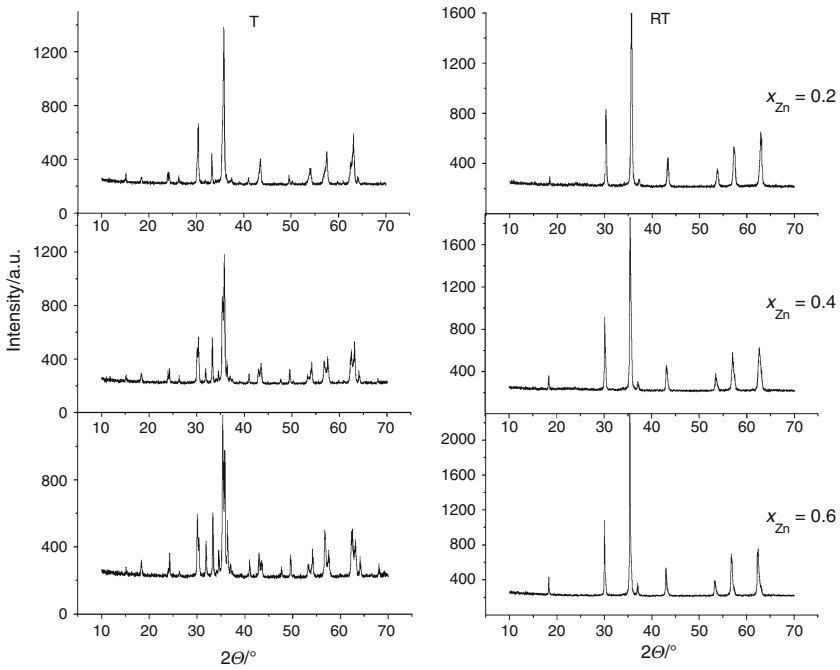


**Fig. 1** XRD patterns of the mixtures ferritized in the T and RT annealing regimes for $T_{ann} = 700$ °C and $t_{ann} = 120$ min

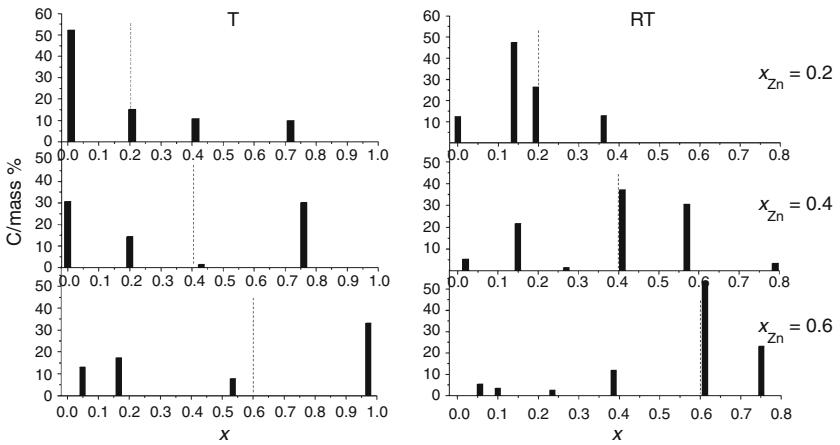


**Fig. 2** *Bar charts* of the phase composition of mixtures ferritized in the T and RT annealing regimes for $T_{ann} = 700$ °C and $t_{ann} = 120$ min

Ferritization in an electron beam yields qualitatively different result. First, the main phases are grouped around the initial composition of the mixture. Second, the concentrations of monoferrite phases have much lower values in comparison with their concentrations after thermal annealing. This testifies to the fact that for the most part, the formation of monoferrite phases had been completed under conditions of RT annealing, and synthesis has passed to the stage of transformation of monoferrites into their solid solutions with the formation of phases of preset composition.

The XRPA results are confirmed by the data of thermogravimetric measurements. To analyze the DTG(M) curves, we took advantage of the results presented in [9] where DTG(M) peaks of lithium–zinc ferrite spinels were identified. In particular, it was demonstrated that the high-temperature DTG(M) peak at 630 °C was due to the magnetic phase transition in lithium pentaferrite at the Curie temperature, and the low-temperature peaks of the DTG(M) curves were due to the same transitions in lithium ferrospinels doped with zinc. Moreover, the position of the maximum and the widths of the low-temperature peaks depended on the zinc concentration in the compound, namely, the intensity of the maximum decreased with increasing zinc concentration and its position was displaced toward lower temperatures.

A comparison of the DTG(M) T and RT curves of the synthesized samples (Fig. 3) demonstrates that the feature in common for both types of synthesis is the presence of the pentaferrite phase and its peak at 630 °C. For identical tendencies of decreasing intensity of this peak with increasing zinc content, the peak intensity $J_{630}$ after T annealing was much greater than after RT ferritization. A decreasing

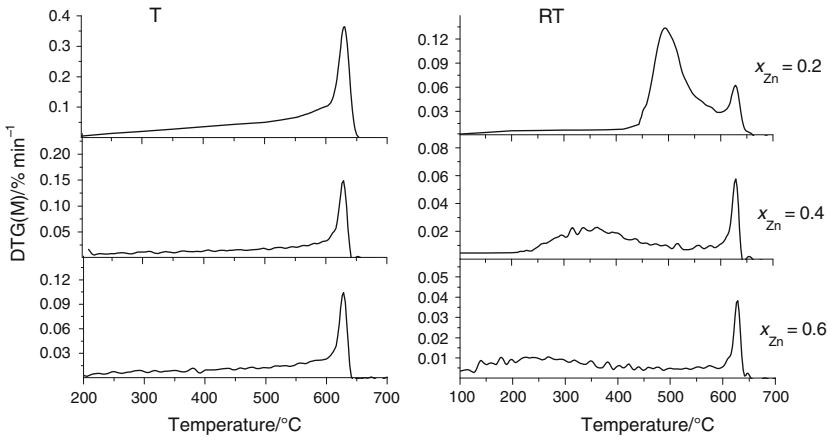


**Fig. 3** DTG(M) curves of mixtures ferritized in the T and RT annealing regimes for $T_{ann} = 700$ °C and $t_{ann} = 120$ min

character of the dependence of $J_{630}$ on $x_{Zn}$ is explained by the fact that, according to the $Li_{0.5(1-x)}Zn_xFe_{2.5-0.5x}O_4$ stoichiometry, a decrease in the lithium oxide concentration is accompanied by the increase in the zinc oxide concentration. Therefore, the amount of monoferrite phase produced from lithium oxide will also decrease. It is obvious that in the initial stage of synthesis, $Li_{0.5}Fe_{2.5}O_4$ lithium pentaferrite is exactly this phase of the initial state of synthesis.

Lower $J_{630}$ values after RT annealing are caused by the lithium pentaferrite phase consumed for the formation of lithium–zinc ferrospinel phases. This is confirmed by the occurrence of clearly pronounced DTG(M) peaks. During T ferritization, despite identical annealing periods and temperatures, the lithium–zinc ferrite phase was absent almost completely. And only a small increase in the low-temperature background at 630 °C could be interpreted as a presence of an insignificant amount of mixed ferrite spinels.

It should be noted that the low-temperature peak amplitude cannot be used to judge the relative fractions of lithium–zinc ferrite spinel phases with different zinc contents. This is due to the fact that the peak intensity is determined by the phase magnetization. However, the saturation magnetization of lithium–zinc ferrite spinels is a complex function of $x_{Zn}$. This fact is a consequence of the Néel theory according to which the diamagnetic replacement of the tetrahedral iron cations by the zinc ions in the region of small concentrations increases the domain magnetization; however, the intersublattice exchange interaction strongly decreases for $x_{Zn} > 0.3$, the magnetic moments in domains are partly disoriented, and the magnetization of the mixture correspondingly decreases [12]. Thus, from the curves shown in Fig. 3 it is impossible to consider that the concentration of the lithium–zinc ferrospinel for the composition with $x_{Zn} = 0.2$ is much greater than the concentration of phases for the composition with $x_{Zn} = 0.6$. For the same reason, it is impossible to judge the relative fractions of the doped and undoped phases from the ratio of the intensities of high- and low-temperature peaks of the DTG(M) curve. However, to elucidate the relative phase fractions, it is quite correct to compare the peaks with identical positions of the temperature maxima, because the equal Curie temperatures testify to close chemical compositions of phases being compared.

## Conclusions

The set of experimental data presented here demonstrates that synthesis with electron irradiation, unlike thermal annealing for identical annealing temperatures and times, results in practically complete transformation of the mixture of reagents into the spinel phases, irrespective of the initial zinc concentration in the mixture. Under conditions of thermal annealing, the main spinel products are phases whose chemical compositions are close to lithium and zinc monoferrites. Ferritization in an electron beam, for the same annealing regimes, results in the formation of lithium–zinc ferrite spinels whose chemical compositions are grouped near the composition of the initial mixture.

Despite an extremely unfavorable annealing regime of powder mixture of reagents—low annealing temperature ($T_{ann} = 700$ °C), insignificant duration of process ($t_{ann} = 120$ min), absence of intermediate mixing—the process of ferritization in an electron beam reaches the stage of lithium–zinc ferrite monophase formation. Under the same conditions of thermal annealing, ferritization proceeds in the initial stage of forming simple monoferrites. This radical difference in phase compositions of ferritized mixtures does not allow their homogeneity to be compared. However, at the same time, the fact of substantial increase in the controllable diffusion interaction among monoferrite phases under high-power electron irradiation can be considered obvious. As a result of this interaction, the rate of lithium–zinc ferrite phase formation increases. In the examined limits of $x_{Zn}$ changes, the zinc concentration had no effect on the observed effects.

## References


1. Ahniyaz A, Fujiwara T, Song S-W, Yoshimura M. Low temperature preparation of $\beta$-$LiFe_5O_8$ fine particles by hydrothermal ball milling. J Solid State Ionics. 2002;151:419–23.
2. Cook W, Manley M. Raman characterization of $\alpha$- and $\beta$-$LiFe_5O_8$ prepared through a solid-state reaction pathway. J Solid State Chem. 2010;183:322–6.
3. Berbennia V, Marinia A, Matteazzib P, Riccerib R, Welhamc NJ. Solid-state formation of lithium ferrites from mechanically activated $Li_2CO_3$–$Fe_2O_3$ mixtures. J Eur Ceram Soc. 2003;23:527–36.
4. Yasuoka M, Nishimura Y, Nagaoka T, Watari K. Influence of different methods of controlling microwave sintering. J Therm Anal Calorim. 2006;83:407–10.
5. Lyakhov NZ, Boldyrev VV, Voronin AP, Gribkov OS, Bochkarev LG, Rusakov SV, Auslender VL. Electron beam stimulated chemical reaction in solids. J Therm Anal Calorim. 1995;43:21–31.
6. Surzhikov AP, Pritulov AM, Ivanov YF, Shabardin RS, Usmanov RU. Electron-microscopic study of morphology and phase composition of lithium–titanium ferrites. Russian Phys J. 2001;44:420–3.
7. Surzhikov AP, Pritulov AM, Lysenko EN, Sokolovskiy AN, Vlasov VA, Vasendina EA. Calorimetric investigation of radiation-thermal synthesized lithium pentaferrite. J Therm Anal Calorim. 2010;101:11–3.
8. Surzhikov AP, Sokolovskiy AN, Vlasov VA, Vasendina EA. Synthesis of lithium–zinc ferrite in bunch of accelerated electrons. Rare Metals Spec Issue. 2009;28:418–20.
9. Surzhikov AP, Lysenko EN, Vasendina EA, Sokolovskii AN, Vlasov VA, Pritulov AM. Thermogravimetric investigation of the effect of annealing conditions on the soft ferrite phase homogeneity. J Therm Anal Calorim. 2010 [Online First].
10. Lin DM, Wang HS, Lin ML, Lin MH, Wu YC. TG(M) and DTG(M) techniques and some of their applications on material study. J Therm Anal Calorim. 1999;58:347–53.
11. Shiliakov SM, Maltsev VI, Ivolga VV, Naiden EP. Atomic structure of lithium–zinc–iron spinels. Reference Izvestiya Vysshikh Uchebnykh Zavedenii, Moskva.Ser.: Fizika; 1977. pp. 111–116.
12. Gorter EW. Saturation magnetization and crystal chemistry of ferrimagnetic oxides. J Philips Res Rep. 1954;9:295.